Journal of University of Science and Technology Beijing
Vol.8(2001), No.3, p.198

Materials

Fabrication and Microstructure of W/Cu Functionally Graded Material

Yunhan Ling, Jiangtao Li, Zhangjian Zhou, Changchun Ge

Laboratory of Special Ceramics & Powder Metallurgy, University of Science and Technology Beijing, Beijing 100083, China
(Received 2000-11-12)

Abstract: W/Cu functionally gradient material (FGM) has excellent mechanical properties since it can effectively relax interlayer thermal stresses caused by the mismatch between their thermal expansion coefficients. W/Cu FGM combines the advantages of tungsten such as high melting point and service strength, with heat conductivity and plasticity of copper at room temperature. Thus it demonstrates satisfactory heat corrosion and thermal shock resistance and will be a promising candidate as divertor component in thermonuclear device. Owing to the dramatic difference of melting point between tungsten and copper, conventional processes meet great difficulties in fabricating this kind of FGMs. A new approach termed graded sintering under ultra-high pressure (GSUHP) is proposed, with which a near 96% relative density of W/Cu FGM that contains a full distribution spectrum (0–100%W) has been successfully fabricated. Suitable amount of transition metals (such as nickel, zirconium, vanadium) is employed as additives to activate tungsten's sintering, enhance phase wettability and bonding strength between W and Cu. Densification effects of different layer of FGM were investigated. Microstructure morphology and interface elements distribution were observed and analyzed. The thermal shock performance of W/Cu FGM was also preliminarily tested.

Key words: tungsten; copper; sintering; functionally graded material; composite

[*This work was financially supported by China National Committee of High Technology New Materials under grant No.863-715-011-0230.*]

1 Introduction

Functionally gradient material (FGM), in which the composition and microstructure vary continuously from one side to another, was first proposed by Japanese scientists as a method to relax thermal stresses caused by a difference in the thermal expansion of the materials used [1]. Materials exposed to high heat flux, such as the first wall and divertor of fusion reactor, whose surface is irradiated by plasma, ion beams, electron beams, etc. when plasma disruption and vertical displacement event take place, and the remainder is forcibly cooled by water, are required to possess the characteristics of both a high thermal erosion-resistance and a good thermal conductivity for the enhancement of the cooling property.

For the highest sputtering threshold of all possible candidates, tungsten will be the most likely armor materials in highly located plasma-interactive components of fusion reactors due to its high plasma resistance [2]. But the joint of refractory tungsten to copper as heat sinks meets a series of difficulties, one of which is the mismatch of thermal expansion coefficients and other properties between two joined materials. **Table 1** shows the main properties of W and Cu.

Table 1 Main physical properties of W and Cu (at room temperature)

Materials	Density / ($g \cdot cm^{-3}$)	Melting point / K	Thermal expansion cofficient / ($10^{-6} \cdot K^{-1}$)	Thermal conductivity / ($W \cdot m^{-1} \cdot K^{-1}$)	Electric resistivity / ($\times 10^{-6} \Omega \cdot m$)	Poisson ratio
W	19.3	3 673	4.5	145	550	0.28
Cu	8.9	1 356	17	400	1.72	0.33

In this paper, the idea of FGM is adopted instead of conventional coating or W-Cu brazing, it is anticipated that a new effective process for fabricating W/Cu FGM with full compositional spectrum will be developed.

Due to the large difference in melting point between W and Cu, it is not easy to fabricate this kind of FGM. The existing processes so far are largely focused on the forming of W skeleton and then infiltrating Cu [3–6]. However, these processes face many obstacles that need to be overcome. These include mutual insolubility of W and Cu, which hinders liquid phase sintering, shrinkage and distortion in the pre-sintering and infil-

tration processes requiring expensive machining [7], and inhomogeneous Cu distribution, porosity, and impurities causing deleterious effects on the electrical/thermal conductivity of the product. In present work, the possibility of fabricating W/Cu FGM, in which possesses a distinct electrical resistance distribution and thus by graded sintering under ultra-high pressure (GSUHP) is explored. Various means were used to characterize the sintering effects of W/Cu FGM, with emphasis on the relative density and microstructure analysis.

2 Experimental

According to the distinct resistivity between W and Cu, it can be expected that a gradual resistance distribution and thus a elevated temperature zone will be constructed when strong electric current passes through FGM green sample along their compositional variation direction (from Cu to W). By controlling the resistance distribution and current density input, graded sintering of FGM,which is characteristic of large melting point such as W and Cu, may be feasible. However, Ultra-high pressure is required for shortening sintering time to inhibit macro diffusion of components in FGM.

A special experimental setup was designed to fabricate W/Cu FGM, which is shown in **figure 1**. This device consisted of a mechanical press, pressure vessel and associated electrical and hydraulic system. FGM assembly, which contained W/Cu FGM green compact, was placed in the pressure vessel. The pressure was applied by raising the bottom anvil with force provided by lower hydraulic ram. The sample assembly was encapsulated in pyrophyllite sleeve, which acted as heat/electric insulator in graded sintering. Graphite and steel platelet were used as sealing and pressure-transferring components respectively as well as electric conductor.

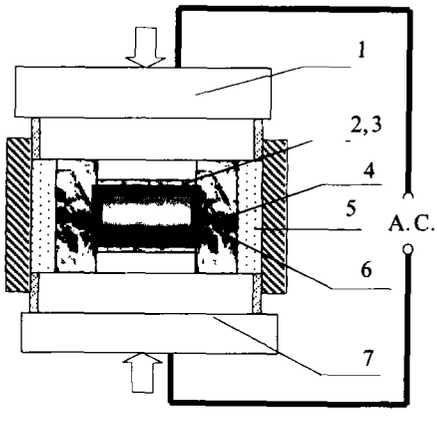

Figure 1 Schematic illustration of experimental setup, 1—upper anvil; 2,3—steel and graphite platelet; 4—FGM green sample; 5— pressure vessel; 6—pyrophyllite sleeve; 7—bottom anvil.

The alternating current (A.C.) passed through and the FGM green compact was heated mainly by conduction.

W powder with average particle size of 3 μm, purity of more than 99% and Cu powder with particle size of −74 μm, purity of >99% were used. In order to activate W sintering and enhance bonding strength between W and Cu, 2%Ni and 10%Zr or 10%V (mass fraction) were introduced in W and Cu powder, respectively. W and Cu powders were mixed and milled with different volume ratio according to the design of compositional distribution in the graded layers of the FGM: $C=(\frac{x}{d})^p$, where C is the volume fraction, x the relative distance from the surface, d the thickness of the FGM layer, and p the compositional distribution factor. In this work, experiments on full composition spectrum (0–100%W) of 6-layered W/Cu FGM with $p=1$ were conducted. Then, powders with different composition were stacked layer by layer in a steel mould to form green compact of ϕ20 mm×10 mm.

Graded sintering was performed under the pressure of 5 GPa, electric power input was about 13 kW (7V, 1 850 A) and sintering time was 40 s. The density of sintered W/Cu FGM was measured by Archimedes' method, and the structure was examined by SEM. The thermal shock resistance property of W/Cu FGM was preliminarily evaluated by cyclic impact of laser pulse.

3 Results and Discussion

3.1 Densification effects

When strong current passed through the W/Cu FGM green compact, a gradient temperature distribution was quickly established; the highest temperature was at W side. Owing to its high thermal conductivity and surface radiation energy, it can be inferred that a part of heat will be conducted to Cu side, as a result, the densification should be expected to be increased from monolithic W to Cu side for their large melting point gap (about 2 300 ℃). But it is not always that case, as seen from **figure 2**. The densification drops at 2nd layer (20% Cu, volume fraction), which may be caused by high temperature compared with the melting point of copper that lead to the partial evaporation of Cu or liquid Cu dispelling from W matrix, this phenomenon was also reported in reference [8]. Low density at copper layer may be caused by insufficient heat transfer for short sintering duration, while less densification at monolithic W layer was most probably attributed to its low heat reserved and less pore removal.

The relative density of W layer is more than 93.5%. For using zirconium binder, the density of overall W/

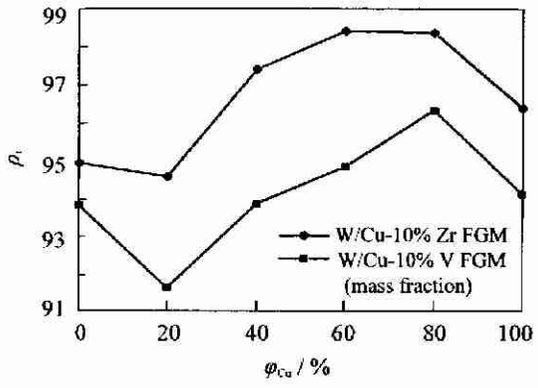

Figure 2 Relative density (ρ_r) of different layer vs. copper content (φ_{Cu}, volume fraction).

Cu FGM is 13.46 g/cm^3, which is 95.5% of its theoretical density (14.1 g/cm^3), while using vanadium, the density is 13.22 g/cm^3, 94.47% of its full density (13.96 g/cm^3). The lower density of W/Cu FGM using V as binder is probably due to its higher melting point (2 163 ℃) compared with that of Zr (1 850 ℃). According to binary phase diagrams of Cu alloy, Cu-10%V (mass fraction) alloy also has a higher melting point than that of Cu-10%Zr alloy.

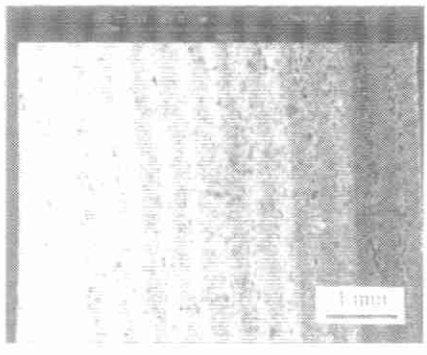

Figure 3 Backscattering image (BSI) of overall 6-layered W/Cu FGM.

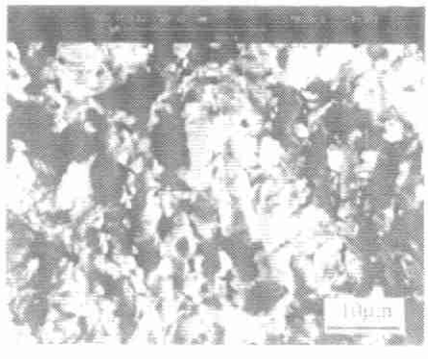

Figure 5 BSI of 80% W layer (volume fraction).

3.3 Interface investigation

W/Cu FGM is a hybrid composite, and W and Cu are immiscible, they can only form pseudo alloy, whose bonds may be poor on service. The improvement should focus on introducing phase binder, which can form solid solution with both W and Cu. It should be pointed out that compounds reacted by binder and major phases in most case are harmful.The binder selection always depends on the analysis of binary or ternary system diagrams. **Figure 9** displays XRD patterns of each layer of W/Cu FGM, where nickel was used as phase binder, it is evident that no interface reaction appears during rapid GSUHP. However, macroscopic XRD analysis can-

3.2 Microstructure analysis

Figures 3–8 show the details of SEM morphology for W/Cu FGM. **Figure 3** depicts the overall 6-layered FGM backscattering image and a good graded compositional transition is noticeable, which reflects no macro elemental migration during short time sintering. **Figure 4** demonstrates relatively good sintering of monolithic W layer, W particles were melted and bonded together. However, a portion of residual pores remained, which was possibly caused by the absorbed gases in primary powders, which could not easily be eliminated under ultra-high pressure and short duration of sintering. **Figures 5–7** present SEM of 80%, 60% and 20% W (volume fraction) layer, respectively, it can be seen that isolated W particles increase as a function of copper content, in 80%Cu (volume fraction) layer almost no W particle sintered each other and just dotted as dispersoid in copper matrix. The average particle size of isolated W remains about 3 μm, no obvious grain growth was observed. **Figure 8** is SEM of Cu layer; pits and vacancies are still found, which is also the home to binder phase.

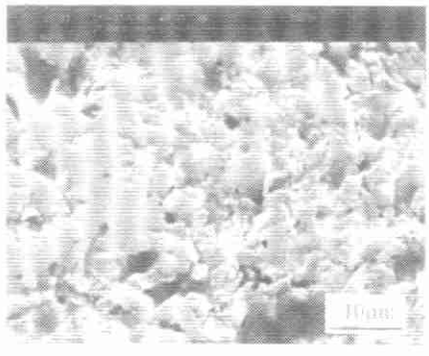

Figure 4 SEM of W layer.

Figure 6 BSI of 60% W layer (volume fraction).

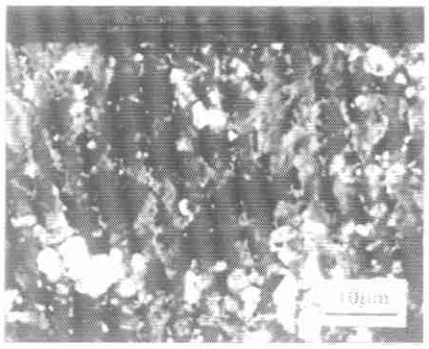

Figure 7 BSI of 20% W layer (volume fraction).

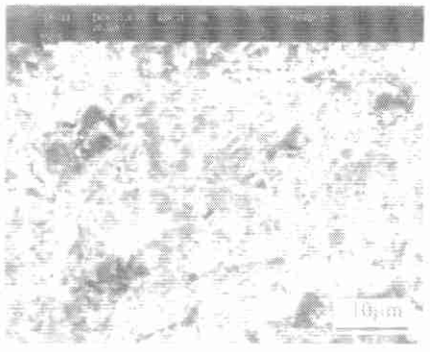

Figure 8 SEM of Cu layer.

Figure 9 X-ray diffraction patterns of different layer of W/Cu-10%Ni (volume fraction) FGM.

not judge the actual bonding of binder and the major phase of FGM. **Figure 10** delineates the SEM of W layer. It can be seen that nickel is well melted and spread on the surface of W boundary; this is beneficial for W particles' rearrangement during initial sintering stage. From **figures 11** and **12**, it can seen that inter-diffusion between W and Ni exists conspicuously despite their transient sintering under ultra-high pressure; the thickness of inter-diffusion layer is more than 5 μm, which is conducive to W sintering.

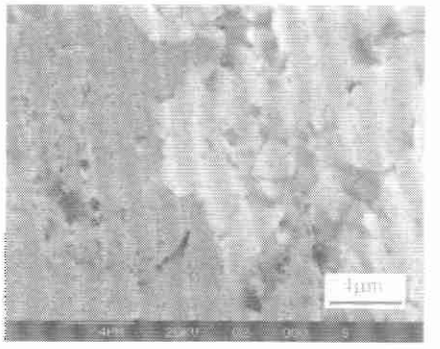

Figure 10 BSI of W-Ni interface.

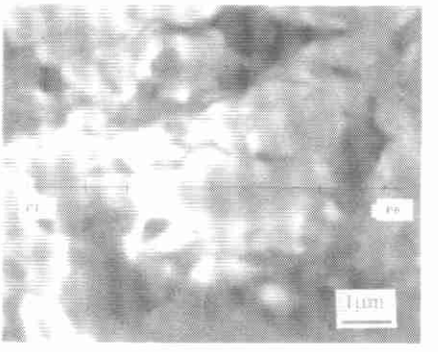

Figure 11 SEM of W layer.

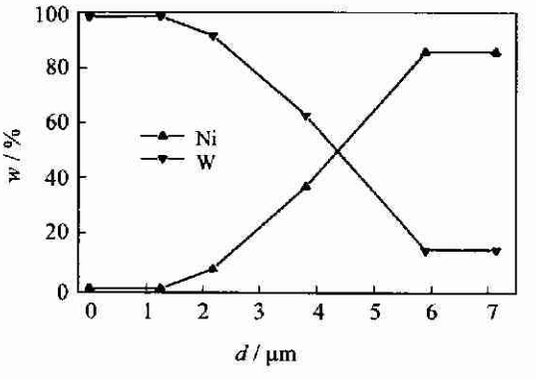

Figure 12 Elemental distribution of W-Ni interface (*w*: element mass fraction; *d*: distance from point 1).

Figures 13 and **14** exhibit the relations among W, Zr and Cu. As a binder, Zirconium reveals very good wettability against W and Cu. EDS dot-map also revealed slightly Zr diffusion in dominant phases of W and Cu.

3.4 Mechanism of graded sintering

Before sintering, when ultra high pressure is applied to W/Cu FGM green sample, the stage of particle sliding, crushing and plastic transforming will be finished soon.

Because of their large disparity in melting points between W and Cu, the mechanism can be categorized into two types. One is for refractory tungsten; another is for copper rich composition. In W layer, plastic flow and volume diffusion mechanism may be dominant for lack of liquid phase during sintering, as seen from figures 10–12, the melted nickel spreads on the surface of

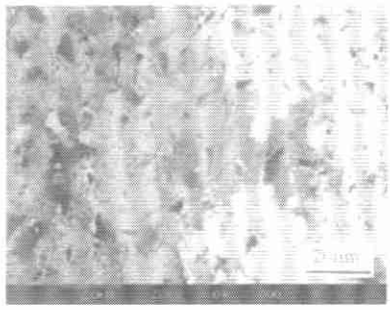

Figure 13 BSI of W-Zr-Cu ternary area.

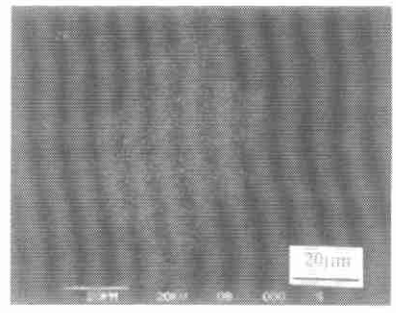

Figure 14 EDS dot-map of Zr distribution of figure 13.

W matrix, with which micro-flow (rearrangement) of W particles can proceed. Inter-diffusion between W and Ni further activate W sintering. As we know, the solubility of W in Ni is appreciable (10–20%), while Ni in W is negligible, so the diffusion rates of W and Cu are different. W atoms penetrate continuously into Ni, leading to the close combination of W particles and a number of vacancies or micro-pores on the surface of W particle. Defects in crystal lattices caused by inter-diffusion are conducible to material migration and plastic flow of W particles. Diffusion is always the rate-controlling step of sintering process, as a result, short duration and pressurized gas in primary powders may hinder densification. As for copper rich layer, viscous flow may be the major sintering mechanism for its relatively low melting point and good plasticity of copper at room temperature.

3.5 Thermal shock performance

Thermal shock experiment for W/Cu FGM was performed in the air by cyclic impact of laser pulse on W surface. SEM and mass loss rate were employed to characterize and evaluate the hot impact consequence. The experimental conditions are as follows:

Pulse width: 4 ms;

Pulse frequency: 10 Hz;

Dot diameter: 0.72 cm;

Energy density: 123 MW/m^2;

Cyclic times: 200 times.

The examination of the morphology on W surface of W/Cu FGM showed that no obvious structural damage but oxidation layer was found on the surface. The mass loss rate of the overall W/Cu FGM is $-0.21\ mg \cdot cm^{-2}$, which means the mass loss of that sample is increasing after laser impact. The increase is ascribed to the oxidation of metals of W and Cu matrix in the air due to the temperature rise of the whole sample.

The preliminary result of thermal shock performance of W/Cu FGM reveals its promising application as divertor component that might be survived under normal service conditions, of which peak heat fluxes are less than $20MW/m^2$ [9].

4 Conclusions

(1) A novel approach termed grade sintering under ultra-high pressure (GSUHP) is proposed, with which a near 96% relative density of W/Cu FGM that contains a full composition spectrum (0–100%W) has been successfully fabricated on condition of 5 GPa pressure applied and 13 kW power input for 40 s.

(2) Using zirconium as phase binder, the relative density of W/Cu FGM is greater than that of using vanadium.

(3) Microstructure analysis showed that a good graded composition of W/Cu FGM had been obtained; no chemical reaction among W, Ni and Cu, and a more than 5 μm thickness of W-Ni inter-diffusion layer was observed during rapid GSUHP.

(4) Preliminary thermal shock test demonstrated that W/Cu FGM could survive without obvious structural damage after 200 times cyclic impact of laser pulse with an energy density of $123\ MW/m^2$.

References

[1] M. Niino, T. Hirano, R. Watanabe: *J. Jpn. Soc. Compos. Mater* (In Japanese), 13 (1987), No. 6, p. 257.

[2] I. Smid, M. Akiba; G. Vieider, et al: *J. Nuclear Materials*, 258-263 (1998), p. 160.

[3] M. Takahashi; Y. Itoh; M. Miyazaki, et al.: *Int. J. of Refractory Metals & Hard Materials*, 12 (1993-1994). p. 243.

[4] Y. Itoh, M. Takahashi; H. Takano: *Fusion Engineering and Design*, 308 (1996), P. 279.

[5] R. Jedamzik; A. Neubrand; J. Rodel: *Materials Sci. Forum*, 308-311 (1999), P. 782.

[6] U. Birth; M. Joensson; B. Kieback: *Materials Sci. Forum*, 308-311 (1999), P. 766.

[7] J. L. Johnson, R. M. German: *Pro. PM2 Tec*, 1993, Nashville, TN, USA, May 1993, Metal Powder Industries Federation, vol. 4. p. 201.

[8] S. Yoo, M. S. Krupashankara, T. S. Sudarshan, et al.: *Materials Science and Technology*, 14 (1998), No. 2, p. 170.

[9] ITER-FEAT Outline Design Report. ITER Meeting, Tokyo, January 2000, p. 28.